Coordinated predictive control in active distribution networks with HV/MV reactive power constraint

J.MORIN, F.COLAS
Arts et Métiers ParisTech
L2EP
Lille, France
juliette.morin@ensam.eu
frederic.colas@ensam.eu

S.GRENARD
Enedis
Paris, France
sebastien.grenard@enedis.fr

J-Y. DIEULOT
Polytech Lille
CRIStAL
Lille, France
jean-yves.dieulot@polytech-lillefr

X. GUILLAUD
Ecole Centrale de Lille
L2EP
Lille, France
xavier.guillaud@ec-lille.fr

***Abstract*—This paper presents a new real time centralized Model Predictive Control algorithm for distribution networks. Compared to existing works regarding MPC volt var control, the proposed algorithm controls not only the MV voltages but also the reactive power exchange at the distribution and transmission systems interface. Control of reactive power exchange is a new requirement of the European Network Code on Demand and Connection. The controller adjusts the reactive power of the distributed generators and the voltage reference of HV/MV on load tap changers and capacitor banks. This method was simulated on a 20 kV network taking into account actual technical limitations of distribution networks.**

***Index Terms*— Distribution Network, Model Predictive Control, Reactive Power Management, Smart Grids, Voltage Control**

I. Introduction

The Traditional use of Volt/Var Control (VVC) schemes in distribution networks using transformers with On Load Tap Changers (OLTC), capacitor banks (CB) could be no longer sufficient to mitigate voltage rises.. Indeed, the insertion of distributed generation and the replacement of Medium Voltage (MV) overhead lines by underground cables raise new operational concerns in MV networks. A high level of MV underground cables along with low power consumption could lead to reactive power flowing upwards from MV networks to High Voltage (HV) networks, contributing to increase transmission grid voltages [1] and leading to the saturation of some existing HV/MV transformers' OLTC [2]. This trend could also become a concern with the new requirements included in the draft of the European Network Code on Demand Connection (DCC)[1]. According to this code, new distribution networks installations connected to transmission networks are required to have the capacity to restrain reactive power flows towards transmission systems, especially at low active power consumption.

In order to deal with these new operational constraints and keep increasing the level of Distributed Generations (DG) penetration in distribution networks, one can consider two main approaches that should be combined together: real-time control and/or grid reinforcement. The topic of real-time voltage control for distribution network in presence of DG has been extensively studied and there exists a substantial literature proposing a variety of methods [3]. Most of recent works focus on coordinated voltage control based on optimal control strategies through a global controller. A particularly attractive approach is the Model Predictive Control (MPC) [4]–[6] which consists of an optimal multi-step algorithm that can deal with various constraints, time delays and can anticipate predictable disturbances. The receding horizon approach allows the system to track smoothly the desired state, as the introduction of slack variables helps to handle constraints infeasibility whenever needed. Then, contrary to single-step approaches, inaccuracies in the models (usually based on sensitivity matrices and constant load models) can be accounted for through this closed-loop approach.

However, the issue of reactive power exchanges at DSO-TSO interface is not addressed in MPC real-time VVC except in [7], where the authors propose to integrate a constraint either on voltage or reactive power at the HV side of the transformer with a MPC approach. Moreover, in MPC VVC there is no fair coordination between actuators since OLTCs are not properly integrated in the prediction horizon. For instance, OLTCs are handled as known perturbation assuming that the DG active and reactive powers are the most expensive actions [4]. In [6], the OLTC is not considered in the MPC formulation, a tap change is triggered only in case of infeasibility.

Next the infrastructures required for most of the controls in literature are far from the nowadays technical state of the art solutions used in distribution networks and from the present level of DG penetration. However European Grid Codes requirements consider nowadays networks. In this paper, simulations have deliberately been conducted considering current technical solutions. Since the approach is rather flexible, the proposed control algorithm can be easily adapted to distribution networks with more actuators and flexibilities.

This paper proposes a new real-time multi-objective MPC based controller suitable for short-term future distribution systems. Control variables are reactive power of DG, voltage reference of OLTC and CB. They are used locally to manage

[1] Network Code on Demand Connection, ENTSO-E, 21 December 2012. available at https://www.entsoe.eu/resources/network-codes/demand-connection

978-1-5090-3358-4/16/$31.00 ©2016 IEEE

the voltage, and in a coordinated manner, to achieve the common objective of regulating the reactive power flows towards the HV network by controlling the power factor. Part II is dedicated to the presentation of the MPC algorithm.

This paper is structured as follows: first the objectives and the model of the system are presented. Then, the formulation and resolution of the MPC problem are explained. Test beds, industrial requirements, results and conclusions are presented in Part III, IV and V.

II. COORDINATED PREDICTIVE VVC

As aforementioned, a Model Predictive Control approach has been used in this work. The principle consists in solving on-line a finite horizon open-loop problem at each sampling time, knowing the current and predicted states of the system [8]. A sensitivity model is used herein to predict the future states of the system over a prediction horizon consisting of N_p steps. At each instant *t,* the controller evaluates an optimal control sequence of *N* elements:$[\Delta u(t), \dots \Delta u(t + k\, t_s), \dots \Delta u(t + (N-1)t_s)]$. Then, only the first element $\Delta u(t)$ is applied; t_s is the sampling time on the control horizon *N*. The whole process is then repeated once a new set of measurements is available to update the prediction. Control and prediction horizons are receding, and the duration of the prediction horizon must be at least equal to the duration of the control horizon. In the sequel, length of prediction and control horizons are supposed to be equal to *N* and $x(k) = x(t + kt_s)$.

A. Voltage control with reactive power exchange limitation

The system to be controlled is a radial MV distribution network with distributed generation. The existence of OLTC and CB at the HV/MV substation is also assumed. The objectives of the proposed schemes are twofold:

1/ The first objective is to maintain the MV voltages inside a target band. This band can correspond to contractual limits which are [0.95, 1.05] p.u. for the French distribution network.

2/ The second one regards the control of the reactive power exchange at the DSO-TSO interface by maintaining the ratio of reactive power over active power consumed by the MV network at this interface inside a range of predefined values. This targeted range of values can be defined by the TSO in accordance with the DSO. This ratio will be designated by $\tan(\varphi)_{HV\to MV} = \frac{Q_{HV\to MV}}{P_{HV\to MV}}$ in the sequel. This is a "common good" goal that requires coordination between actuators. Coordination is also useful to insure that both objectives can be reached.

B. Modelling of the system

In order to meet the double objectives, the control variables correspond to the OLTC tap change ($n_{OLTC\,ref}$) - by adjusting the voltage reference - the reactive power of DG ($Q_{DG\,ref}$), and the number of activated steps of CB ($n_{CB\,ref}$) as shown in Fig. 1. Some papers consider to use as well the active power of DG which can raise contractual and economic difficulties. Thus the contribution of DG was limited to reactive power adjustment, but the proposed algorithm can be easily adapted. The measured variables are the voltage at every node of the network, active and reactive production of DG, active and reactive power flowing from distribution system to the transmission system and state of CB. The measurement variables do not necessarily coincide with actual measurements but can be the results of a state estimator or from remote signaling, even from topological data from a data center. The regulated variables are the voltage at every node of the MV distribution network (V) and the $(\tan(\varphi)_{HV\to MV})$.

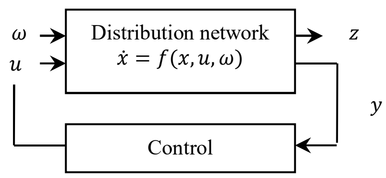

x: state of the system
u: control variables $u = [n_{OLTC\,ref}, Q_{DG\,ref}, n_{CB\,ref}]$
y: measured output $y = [V, P_{DG}, Q_{DG}, n_{CB}, P_{HV\to MV}, Q_{HV\to MV}]$
z: regulated variables $z = [V, tan(\varphi)_{HV\to MV}]$
ω: disturbances

Fig. 1: Control structure

MPC relies on a model to predict and anticipate the future behavior of the output z of the system with respect to the inputs u and y. In this work a common static model based on sensitivity matrices to express the change of the output induced by a variation of control variable has been selected. For the calculation of sensitivity matrices refer to [4], [9], [10]. To be accurate, theses matrices should incorporate the load to voltage relationship which is not well known in practice, here loads have been considered as constant power (but not in the simulation) for this calculation.

Next, the actuators involved in the control exhibit different dynamics: DG and CB acts instantaneously compared to the OLTC that embeds time-delays (classically around 60s). To account for nowadays technical limitations and to insure a proper coordination between these actuators with distinct dynamics, it has been chosen to send a control action every minute: $t_s = 60\ s$.

So, given the ability of MPC to deal with time-delay, the prediction equations are given by (1) and (2):

$$V(k) = V(k-1) + \frac{\partial V}{\partial n_{CB\,ref}} \Delta n_{CB\,ref}(k) + \frac{\partial V}{\partial Q_{DG\,ref}} \Delta Q_{DG\,ref}(k) + \frac{\partial V}{\partial n_{OLTC\,ref}} \Delta n_{OLTC\,ref}(k-1). \tag{1}$$

$$Q_{HV\to MV}(k) = Q_{HV\to MV}(k-1) + \frac{\partial Q_{HV\to MV}}{\partial n_{CB\,ref}} \Delta n_{CB\,ref}(k) + \frac{\partial Q_{HV\to MV}}{\partial Q_{DG\,ref}} \Delta Q_{DG\,ref}(k) + \frac{\partial Q_{HV\to MV}}{\partial n_{OLTC\,ref}} \Delta n_{OLTC\,ref}(k-1). \tag{2}$$

Active power of load and generation is supposed to remain constant within the prediction horizon but is updated every minute. This model is not exact since it doesn't include changes in active and reactive losses induced by a change in voltage or power injections.

C. Predictive control strategy

1) Objective function: minimization of control actions costs

Usually, loss minimization is selected as the objective function for optimal-based control. This can be a relevant choice if accurate estimates of current which highly depend on the load are available. Unfortunately, load models are one of the major sources of uncertainties in power systems simulations and lead to errors in losses estimation [11]. In order to solve operational constraints while minimizing control actions costs, real time control reducing control efforts (and thus maintenance costs) is a good trade-off. Here, to avoid unnecessary changes in control when the constraints are satisfied, the following classical quadratic programming objective function has been used to minimize the control effort:

$$\min_{\Delta u} J = \min_{\Delta u} \sum_{k=0}^{N-1} \Delta u^T R \Delta u(k) \quad (3)$$

R is the actuators cost matrix and allows to discriminate cheap actions from expensive ones. This cost matrix can evolve inside the prediction horizon to account for time-dependent costs.

2) Constraints within the prediction horizon and uncoupling of objectives

One of the major advantages of MPC approach is its ability to deal with various kinds of constraints on states and control variables within a prediction horizon. The double-objective of the control has been integrated in the problem as terminal constraints:

$$V_{min} \leq V(N+1) \leq V_{max}, \quad (4)$$

$$tan(\varphi)_{min} \leq tan(\varphi)_{HV \to MV}(N+1) \leq tan(\varphi)_{max}. \quad (5)$$

Note that the thermal constraints are not included in the problem. Indeed, it has been checked through simulations that the grid is properly designed (regarding thermal constraints) while adjusting the reactive power output of DG inside a predefined range of values.

So, for each actuator, some physical limitations should be taken into account. The latter can be written as:

$$u_{min} \leq u(k) \leq u_{max}, \quad (6)$$

$$\Delta u_{min} \leq \Delta u(k) \leq \Delta u_{max}. \quad (7)$$

These constraints must be satisfied at any cost: no economic trade-off can be found. That corresponds to the limits on the voltage references for OLTC, CB, discrete positions of OLTC and on reactive power outputs of DG. These reactive power limits can vary with several factors such as the active production of the considered DG or even the voltage at their terminals and the technologies used.

In order to specify the trajectory of the controlled variables, a funnel can be defined inside the horizon in which the controlled variables must evolve to reach the final objectives defined by the constraints (4) and (5). An exponential funnel has been chosen and defined as follows:

$$x_{max}(k) = x_{max} - \alpha_x{}^{f(k)}(x_{max} - max(x(k), x_{max})). \quad (8)$$

$$x_{min}(k) = x_{min} + \alpha_x{}^{f(k)}(x_{min} - min(x(k), x_{min})). \quad (9)$$

with :

$$0 \leq \alpha_x \leq 1, \quad (10)$$

$$\alpha_x{}^{f(0)} = 1 \ , \ \alpha_x{}^{f(N+1)} = 0, \quad (11)$$

$$f(k) = k^{\beta}. \quad (12)$$

and x corresponds either to the MV voltages V or to the tangent $\tan(\varphi)_{HV \to MV}$.

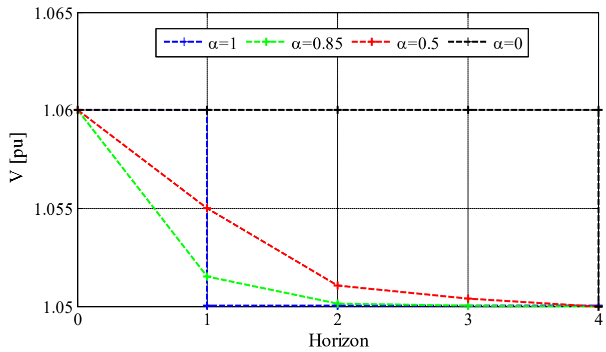

Fig. 2 : Evolution of the exponential funnel on voltage constraints inside the prediction horizon for several value of α and $\beta = 0.001$

Fig. 2 shows the evolution of the exponential constraints for different values of α. The introduction of these constraints allows tuning the speed of convergence. Thus, fast changes with high amplitude of control actions can be avoided. Both objectives can be uncoupled by tuning separately parameters α_V and α_t related to voltage and tangent respectively. This uncoupling is appealing since the dynamic needed for the voltage and the $\tan(\varphi)_{HV \to MV}$ control can differ from each other. This will be further illustrated in part III.

3) Hierarchical relaxation of constraints and infeasibility

It may happen that the problem is not feasible if the objectives are too strict or after a severe disturbances. However the controller should still be able to bring the system as close as possible to a situation respecting every aforementioned constraints: this can be achieved using constraints relaxation, see [4]. The contribution of this work is to prevent the competition between the double objectives of the control and the competition between these and the relaxation of the constraints. To this end, a hierarchical structure has been defined. If the general problem is not feasible:

1/ First a relaxation of the exponential convergence of $\tan(\varphi)_{HV \to MV}$ is considered (constraints (8) and (9), and then constraints (5)), then if the problem is still not feasible the following constraints can be relaxed:

2/ Relaxation of exponential convergence on V (constraints (8) and (9), and then constraints (5)).

The correction of the MV voltages has been considered as the primary goal of the control, while others are secondary objectives and considered only if this primary goal is reached. Since every objective's constraint could be relaxed, theoretically there could be no case of infeasibility. This relaxation is made depending on the priority given by the DSO. Other choices can be made and the hierarchical relaxation is easily modifiable. Practically this relaxation can be done through the use of slack variables ε_{xi} that soften the constraints (4), (5), (8) and (9).

$$x_{min}(k) - \varepsilon_{x1}(k) \leq x(k) \leq x_{max}(k) + \varepsilon_{x2}(k). \tag{13}$$

The use of slack variables $\varepsilon(k)$ is heavily penalized through quadratic penalty on the objective function with the cost matrices S and T as detailed in Table I. The elements of this cost matrix should be set far higher than the coefficients of the cost R which represents actuators change costs.

TABLE I : COSTS FUNCTION ASSOCIATED TO THE RELAXED MPC

MPC	Cost functions	Relaxed constraints
MPC1	$\min_{\Delta u} J_1 = \min_{\Delta u} \sum_{k=0}^{N-1} \Delta u(t+k) R \Delta u(t+k)^T$	-
MPC3	$\min_{\Delta u, \varepsilon_t} J_2 = \min_{\Delta u, \varepsilon_t} (J_1 + \Delta\varepsilon_t(N) T \Delta\varepsilon_t(N)^T + \sum_{k=0}^{N} \Delta\varepsilon_t(k) S \Delta\varepsilon_t(k)^T)$	(8), (9) on tangent (5)
MPC5	$\min_{\Delta u, \varepsilon_t \varepsilon_v,} J_3 = \min_{\Delta u, \varepsilon_t, \varepsilon_v} (J_2 + \Delta\varepsilon_v(N) T \Delta\varepsilon_v(N)^T + \sum_{k=0}^{N} \Delta\varepsilon_v(k) S \Delta\varepsilon_v(k)^T)$	(8), (9) (4), (5)

II. SIMULATION TEST BED AND IMPLEMENTATION

A. Presentation of the 20 kV network

The multi-objective MPC algorithm has been tested through simulations on a 20 kV radial network which is a fictional academic system. It was inspired by the network presented in [6]. Topological data have been kept, as well as the position of loads and generators. This network corresponds to a traditional radial European MV network. Fig. 3 presents its topology and the actuators' location has been highlighted. The maximum active power load corresponds to the 7 p.m. case presented in [12], and a power factor of 0.92848 has been imposed. Some modifications have been made to better match the current French situation.

The three branches have a different type of feeder, each corresponding to the ones existing in France: one with only consumption (in green in Fig. 3), one with both production and consumption (called mixed feeder, in blue) and one with only production ("dedicated feeder", in orange). For load models, a constant impedance model has been assumed for reactive power whereas a constant current was considered for active power. Industrial loads were modeled as small motors. Next, some changes have also been made regarding HV/MV transformers parameters (see Table II).

The OLTC associated to the HV/MV transformer has 17 tap positions ([-8, +8]) with 1.5% voltage per tap. Fig. 3 gives the position and the maximum active power of each DG. The reactive power is controllable inside the range $[-0.35, +0.4]P_{max}$ which corresponds to French regulation limitations.

A CB with three steps of 1.8 MVAR is installed at the secondary side of the HV/MV transformer.

TABLE II: TRANSFORMERS' PARAMETERS

Transformer	Ratio [kV/kV]	S_{nom} [MVA]	Copper losses [kW]	OLTC
HV/MV	62.5/21	36	21	Yes
MV/LV - 1	20/0.4	0.63	6.5	No
MV/LV - 2	20/0.4	0.4	4.6	No
MV/LV - 3	20/0.4	0.25	3.25	No

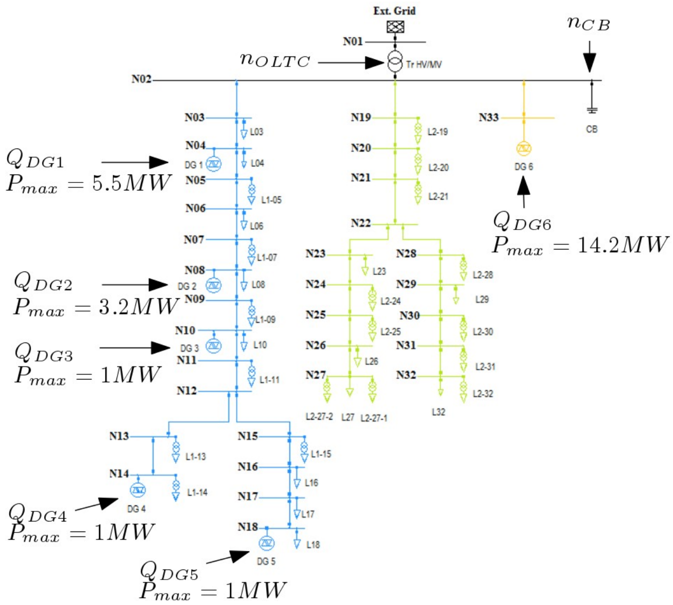

Fig. 3: Network topology

The grid was properly designed without DG3, DG4 and DG5 to meet every DSO requirements. Thus the voltage at every node can remain inside the contractual range of values [0.9, 1.05] p.u. for every load and production scale with only DG1 DG2 and DG6, considering a zero power factor for every DG. In the following simulations, 1 MW is connected to the nodes N10, N14 and N15 (corresponding to DG3, DG4 and DG5 as detailed in Fig. 3). For all of the simulations, a constant sensitivity matrix has been used and was calculated once for a loading scale of 100 % and with 0 % of production. This calculation was performed assuming constant load model.

B. Industrial requirement considerations

It is assumed that the active and reactive powers flowing through the HV/MV transformer are measured locally and retrieved in "real-time" by the Distribution Network Control Center (DNCC) as well as the powers of each DG connected to the MV networks. A new set of measurements is available every minute and consists of an average of 6 actual local measurements taken down every 10 s. Regarding voltage amplitudes, the existence of a state estimator as described in [12] is assumed. In order to reproduce the actual precision of measurement (0.5% for voltage and 1% for power), a

Gaussian white noise has been superimposed to voltage and active/reactive power measurements. The control algorithms are located in the DNCC tools, which are able to send control values to the OLTC, DG and CB. DNCC tools are supposed to have access to general knowledge of the network (topology for instance). There is no need for communication between the local controllers.

C. Choice of MPC parameters

A horizon of $N = 4$ was selected, and the controller is acting every minute $t_s = 60$ s. Regarding the costs, all coefficients of the matrix R are identical, while the coefficients of S regarding the relaxation of constraints (respectively T) are 100 (respectively 1000) time bigger. It is recalled that these costs are configurable and can evolve within the prediction horizon. The parameter β has been set to have $f(1) = \alpha$ and $f(N) = 1.10^{-4}$ (precision on the contraints to be respected at N) $-f$ defined in equation (12). For the convergence speed $\alpha_t = 0.5$ and $\alpha_V = 0.75$ have been chosen. That choice implies that the constraints on voltage inside the horizon are tighter than the constraint on HV/MV reactive power exchange.

III. Results and Discussion

The proposed algorithm has been implemented inside MATLAB using the toolbox YALMIP [13]. The MV network has been simulated with the RAMSES software [14] (RApid Multithreaded Simulator of Electric power Systems) developed by the University of Liège. Two simulations have been carried out in order to explore boundary conditions of the network and are presented hereafter.

A. Case A: 20 % consumption – 100% production

The first case embodies a situation of low consumption along with high DG production. Authorized boundaries for $\tan(\varphi)_{HV\rightarrow MV}$ have been set to [-0.2, 0]. This is a partial choice in order to demonstrate that the controller is able to meet a double-objective and to comply with the potential future requirements of DCC. Indeed, according to this code, whenever the active power consumption (or production) of a distribution network is below 25% of its maximal active power import, the reactive power exchange at the HV/MV networks interface must be inductive.

The controller begins to act at t = 120 s and then acts every 60 s and must correct the voltage and deal with the disconnection of DG6 (in the dedicated feeder) at t = 800 s. Then, a severe disturbance at the transmission side is leading at t = 1500 s to a step increase of 0.08 p.u. in the Thévenin equivalent voltage.

Results can be observed in Fig. 4. The first graph shows the evolution of the voltage (without noises) of two representative nodes in the network plus minimum and maximum voltages. In the second graph, the tangent at the DSO-TSO interface is displayed. The third graph shows the evolution of reactive power output of DG and CB while the evolution of tap position is given in the last graph. From this figure, it can be observed that the controller succeeds to meet its double-objective even after the disconnection and the severe disturbance on the HV side. Using real-time control, the use of the network resources is optimized within the system limitations that are defined by the grid equipment sizing studies to increase the hosting capacity.

Then, several observations can be stated. The reactive power references of DG are still evolving after the correction of voltages due to the presence of noises. However, these variations are very slow and with low amplitude. Although the costs are uniform for every DG, the requested reactive power is not the same. Here, the choice is made depending on the corresponding voltage sensitivity. For instance, DG5 is the most requested to absorb reactive power: indeed, the voltage at its terminal is the highest (1.0792 p.u. at t = 0 s). This repartition depends on the cost matrix R.

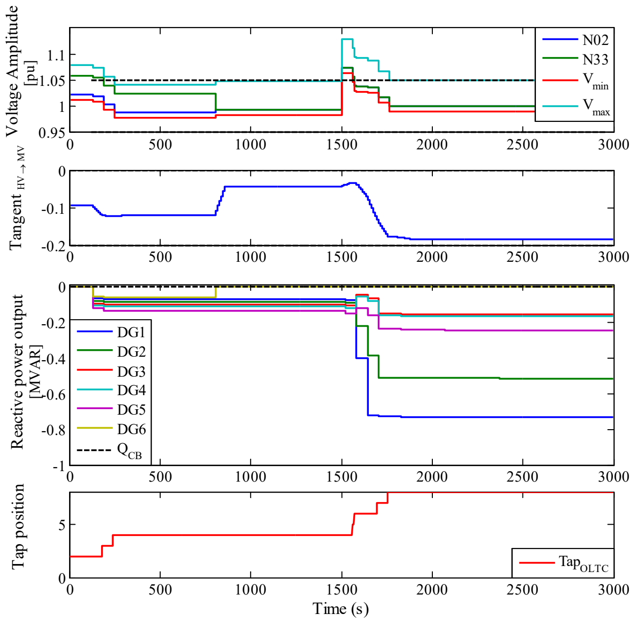

Fig. 4: Results and control, case A

B. Case B: 100 % consumption – 0% production

In the second scenario, the system operates under high active consumption conditions. Some nodes are showing under voltage. Moreover the reactive power exchange between DSO and TSO should be reduced to reach the objective $\tan(\varphi)_{HV\rightarrow MV} = 0$. Once again, after some time, the controller succeeds to meet its double-objective. From Fig. 5, it can be noted that the convergence of the reactive power is slower than the convergence of the MV voltage. Indeed, it takes about 600 s to meet the final objective on reactive power exchange, while only 180 s are needed to correct the voltages. This difference comes from the tuning of parameters α_v and α_t. It proves that the two sub-problems can be dynamically uncoupled. This could be of interest for the DSO since the performance monitoring of voltage and reactive power exchange can be different.

In this test, it can be noticed that the reactive power required by each DG is exactly the same. Indeed, these reactive powers are used to respect the constraint at the TSO-DSO interface. Given that the cost of reactive power is strictly the same for every DG in this theoretical case, the change in reactive power requested by the controller is also strictly equal. No reactive power is requested from the CB. Indeed the reactive power produced by one of the three steps of the CB is about 1.8 MVAR.

Moreover, the controller leaves the tap position of the OLTC constant during the simulation. The natural behavior of the OLTC is bypassed to avoid a non-optimal tap change since using reactive power to adjust the voltage is the cheaper option in this case.

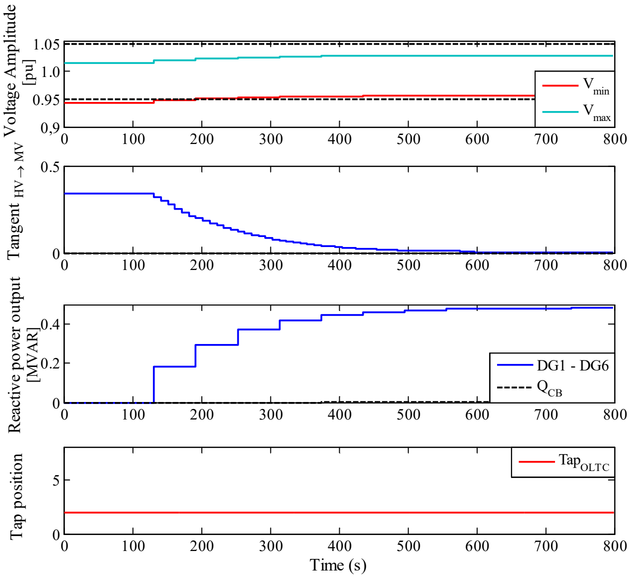

Fig. 5: Results and control, case B

Regarding the execution time, the performance is varying depending on the relaxation of constraints. In the worst case for the simulations presented herein, the execution time is 4.46 s while the minimum time required to solve the optimization problem is 0.176 s. These execution times have been obtained with MATLAB using an i7-2760QM CPU @2.40 Ghz laptop. The control algorithm was not optimized to minimize this execution time since the control is called every minute.

IV. Conclusion

In this paper, an MPC controller has been presented in order to control both the voltages in distribution systems and the reactive power exchange at the Transmission System Operator –Distribution System Operator interface. Thus, this new control strategy could help comply with the new Demand and Connection Grid Codes requirements.

The controller modulates the reactive power output of the Distributed Generators and adjusts the voltage reference of On Load Tap Changer and switch statuses of Capacitor Banks. The flexibility and effectiveness of such a control have been demonstrated through simulations with a 20kV network. The controller can cope with various and evolving situations and succeeds even in the presence of uncertainties in the prediction model and with distorted measurements.

The hierarchical relaxation of constraints prioritizes the different objectives and tackles infeasibility issues. Moreover, the two sub-problems –voltage control and reactive power regulation – can be partially uncoupled by separately tuning the convergence speed of each objective. Special care was taken regarding the industrial requirements of such a control to ensure that it is compatible with nowadays and future distribution networks.

V. Acknowledgements

The authors gratefully acknowledge the contribution of P. Aristidou and T. Van Cutsem (The University of Liège) to this work and especially for the provision of the software RAMSES.

REFERENCES

[1] C. Kaloudas and B. Marshall, "Initial Assessment of Reactive Power Exchanges At Uk Grid Supply Points," in *Proc. CIRED workshop 2014*, 2014, no. 0177, pp. 11–12.

[2] J. Morin, F. Colas, X. Guillaud, and S. Grenard, "Determination and origins of reactive power flows in HV/MV substations," in *Proc. 23rd International Conference and Exhibition on Electricity Distribution (CIRED 2015)*, 2015.

[3] J. Morin, F. Colas, X. Guillaud, S. Grenard, and J.-Y. Dieulot, "Rules based voltage control for distribution networks combined with TSO - DSO reactive power exchanges limitations," in *IEEE Eindhoven Powertech*, 2015.

[4] G. Valverde and T. Van Cutsem, "Model predictive control of voltages in active distribution networks," *IEEE Transactions on Smart Grid*, vol. 4, pp. 2152–2161, 2013.

[5] Z. Wang, J. Wang, B. Chen, M. M. Begovic, and Y. He, "MPC-Based Voltage / Var Optimization for Distribution Circuits With Distributed Generators and Exponential Load Models," in *IEEE Transactions on Smart Grid*, vol. 5, no. 5, pp. 2412–2420, 2014.

[6] M. Farina, A. Guagliardi, F. Mariani, C. Sandroni, and R. Scattolini, "Model predictive control of voltage profiles in MV networks with distributed generation," *Control Engineering Practice*, vol. 34, pp. 18–29, Jan. 2015.

[7] G. Valverde and T. Van Cutsem, "Control of dispersed generation to regulate distribution and support transmission voltages," in *2013 IEEE Grenoble PowerTech*, 2013, pp. 1–6.

[8] E. F. Camacho, D. R. Ramirez, D. Limon, D. Muñoz de la Peña, and T. Alamo, "Model predictive control techniques for hybrid systems," *Annual Reviews in Control*, vol. 34, no. 1, pp. 21–31, 2010.

[9] A. Borghetti, M. Bosetti, S. Grillo, S. Massucco, C. A. Nucci, M. Paolone, and F. Silvestro, "Short-Term Scheduling and Control of Active Distribution Systems With High Penetration of Renewable Resources," *IEEE Systems Journal*, vol. 4, 2010.

[10] Q. Zhou and J. W. Bialek, "Generation curtailment to manage voltage constraints in distribution networks," *IET Generation, Transmission & Distribution*, vol. 1, p. 492, 2007.

[11] A. Ballanti and L. F. Ochoa, "Accepted Paper Assessing the Effects of Load Models on MV Network Losses," in *Australian Universities Power Engineering Conference AUPEC 2015*, 2015, p. p 1–6.

[12] S. Grenard, C. Brolly, O. Devaux, and O. Carré, "Implementation of a centralised voltage control experiment in presence of distributed generation in ERDF's MW network," *CIGRE*, pp. 1–8, 2012.

[13] J. Lofberg, "YALMIP : a toolbox for modeling and optimization in MATLAB," *2004 IEEE International Conference on Robotics and Automation (IEEE Cat. No.04CH37508)*, 2004.

[14] P. Aristidou, D. Fabozzi, and T. Van Cutsem, "Dynamic Simulation of Large-scale Power Systems Using a Parallel Schur-complement-based Decomposition Method," *IEEE Transactions on Parallel and Distributed Systems*, pp. 1–1, 2013.